Published in final edited form as:
J Comp Neurol. 2010 April 1; 518(7): 972–989. doi:10.1002/cne.22258.

Synaptic Maturation of the *Xenopus* Retinotectal System: Effects of Brain-Derived Neurotrophic Factor on Synapse Ultrastructure

Angeliki Maria Nikolakopoulou, **Margarita M. Meynard**, **Sonya Marshak**, and **Susana Cohen-Cory***
Department of Neurobiology and Behavior, University of California Irvine, Irvine, California 92697

Abstract

Synaptogenesis is a dynamic process that involves structural changes in developing axons and dendrites as synapses form and mature. The visual system of *Xenopus laevis* has been used as a model to study dynamic changes in axons and dendrites as synapses form in the living brain and the molecular mechanisms that control these processes. Brain-derived neurotrophic factor (BDNF) contributes to the establishment and refinement of visual connectivity by modulating retinal ganglion cell (RGC) axon arborization and presynaptic differentiation. Here, we have analyzed the ultrastructural organization of the *Xenopus* retinotectal system to understand better the maturation of this synaptic circuit and the relation between synapse ultrastructure and the structural changes in connectivity that take place in response to BDNF. Expression of yellow fluorescent protein (YFP) followed by preembedding immunoelectron microscopy was used to identify RGC axons specifically in living tadpoles. Injection of recombinant BDNF was used to alter endogenous BDNF levels acutely in the optic tectum. Our studies reveal a rapid transition from a relatively immature synaptic circuit in which retinotectal synapses are formed on developing filopodial-like processes to a circuit in which RGC axon terminals establish synapses with dendritic shafts and spines. Moreover, our studies reveal that BDNF treatment increases the number of spine synapses and docked vesicle number at YFP-identified synaptic sites within 24 hours of treatment. These fine structural changes at retinotectal synapses are consistent with the role that BDNF plays in the functional maturation of synaptic circuits and with dynamic, rapid changes in synaptic connectivity during development.

INDEXING TERMS

retinal ganglion cells; BDNF; YFP; immunoelectron microscopy; TrkB; *Xenopus laevis*

Synapse formation is an important step in the establishment of functional neuronal connectivity during development. The selection of potential synaptic partners before functional synapses are formed depends not only on structural but also on functional interactions between developing axons and dendrites at nascent synaptic sites (Lohmann and Bonhoeffer, 2008). Imaging studies have revealed that filopodially mediated contacts between developing axons and dendrites precede synapse formation in the developing brain (Cohen-Cory, 2002; Jontes and Smith, 2000; Lohmann and Bonhoeffer, 2008; Mumm et al.,

*CORRESPONDENCE TO: Susana Cohen-Cory, PhD, Department of Neurobiology and Behavior, University of California, Irvine, 2205 McGaugh Hall, Irvine, CA 92697-4550. scohenco@uci.edu.
Angeliki Maria Nikolakopoulou current address is Center for Molecular Biology and Genetics of Neurodegeneration, Departments of Psychiatry and Neuroscience, Mount Sinai School of Medicine, One Gustave Levy Place, New York, NY 10029.

Additional Supporting Information may be found in the online version of this article.

2006; Wong and Wong, 2000; Yuste and Bonhoeffer, 2004). Thus, synaptogenesis is a dynamic process in which structural changes take place as synaptic circuits mature (Cohen-Cory, 2002). Understanding the relationship between cellular and subcellular synaptic remodelling can consequently shed new light on the functional maturation of a given synaptic circuit.

Because of its relative simplicity, the visual system of nonmammalian vertebrates, such as frogs and fish, has served as an accessible model for exploring the dynamics of synaptic plasticity in the living brain. Imaging and electrophysiological studies in these species have advanced our understanding of the mechanisms by which activity-dependent and molecular signals influence visual circuit development and function (Cline, 2001; Cohen-Cory, 2002; Cohen-Cory and Lom, 2004; Hua and Smith, 2004; Mumm et al., 2006). Important correlates of structural changes in developing axon and dendritic morphology and in synaptic connectivity have been obtained through live imaging of fluorescently tagged synaptic components in individual neurons in both the *Xenopus laevis* and zebrafish visual systems (Alsina et al., 2001; Meyer and Smith, 2006; Niell et al., 2004; Ruthazer et al., 2006). Little is known, however, about how the developing retinotectal system of these two experimental models is organized at the ultrastructural level and how it transitions from an immature to a mature synaptic circuit.

One of the key modulators of synaptic connectivity in the developing and adult vertebrate central nervous system is brain-derived neurotrophic factor (BDNF). BDNF, signaling through its receptor TrkB, can influence the morphological development of neurons as well as their synaptic connectivity, by influencing both synaptic structure and function (Luikart and Parada, 2006; Poo, 2001). In the *Xenopus* visual system, BDNF modulates not only the morphological maturation of presynaptic RGC axonal arbors but also their connectivity, as demonstrated by a number of in vivo imaging studies in which BDNF levels and signaling were manipulated at important stages of retinotectal circuit development (Alsina et al., 2001; Hu et al., 2005; Marshak et al., 2007). Here we have further characterized the *Xenopus* retinotectal system by electron microscopy to understand better how this circuit is organized at two key stages of its synaptic differentiation and to provide a correlate between ultrastructural changes elicited by BDNF and the in vivo dynamic changes in synaptic connectivity previously observed (Alsina et al., 2001; Hu et al., 2005; Marshak et al., 2007). Our results reveal a significant transition from an immature but differentiating neuronal network to a more mature synaptic circuit during a short developmental window, a transition that depends on neurotrophin feedback. Changes in synaptic structure correlate with the developmental period when BDNF expression in this system peaks (Cohen-Cory et al., 1996) and with the expression of the BDNF receptor TrkB at synaptic sites.

MATERIALS AND METHODS

Xenopus laevis tadpoles

Xenopus tadpoles were obtained by in vitro fertilization of oocytes from adult females primed with human chorionic gonadotropin. Tadpoles were raised in rearing solution [60 mM NaCl, 0.67 mM KCl, 0.34 mM $Ca(NO_3)_2$, 0.83 mM $MgSO_4$, 10 mM HEPES pH 7.4, 40 mg/liter gentamycin] plus 0.001% phenylthiocarbamide to prevent melanocyte pigmentation. Tadpoles were anesthetized during experimental manipulations with 0.05% tricane methanesulfonate (Finquel; Argent Laboratories, Redmond, WA). Staging was performed according to Nieuwkoop and Faber (1956). Animal procedures were approved by the University of California Irvine.

Retinal transfection with YFP plasmids and BDNF treatment

To identify RGC axon terminals selectively in the tadpole optic tectum, retinal neurons were transfected with a pCS2$^+$ expression vector coding for yellow fluorescent protein (YFP) under control of the CMV promoter (Marshak et al., 2007). From 0.1 to 0.2 nl plasmid DNA (1 μg/μl) was pressure injected into the eye primordium of stage 20 – 22 anesthetized tadpoles. Tungsten electrodes (Protech International, San Antonio, TX) were positioned across the injected eye, and a train of 10 40-msec square pulses of 45 V was applied to the animals with a CUY 21 electroporator (BEX, Tokyo, Japan). After transfection, tadpoles were reared under filtered illumination, in 12-hour dark/light cycles, until stage 40 – 45, when they were used for experimentation. For ultrastructural analysis and BDNF treatment, tadpoles were screened with epifluorescence illumination for the presence of YFP-labeled RGC axon terminals in the optic tectum, and animals were immediately killed in 1:500 Finquel (stage 40) or reared until stage 45 for BDNF treatment. Briefly, stage 45 tadpoles were microinjected with 0.2 – 1.0 nl vehicle solution or BDNF (200 ng/nl) into the ventricle and caudalmost part of the optic tectum as described previously (Hu et al., 2005). Tadpoles were killed immediately after injection (0 hours; controls only) or 8 or 24 hours after treatment (controls and BDNF).

Antibody characterization

Primary antibodies used in this study are listed in Table 1. Specific information about each antibody is given in this section. A custom-made antibody directed against a 16-amino-acid peptide in the tyrosine kinase domain of *Xenopus* TrkB was obtained from Bethyl Laboratories Inc. (Montgomery, TX). The affinity-purified anti-TrkB polyclonal antibody was raised in rabbits against amino acid residues 396 – 411 (LQNLSKASPVYLDILG) of the cytoplasmic domain of *Xenopus* TrkB. This polyclonal antibody recognizes a band of approximately 110 kDa from stage 45 and adult *Xenopus laevis* brain and eye homogenates by Western blot (Supp. Info. Fig. 1). The band recognized by this antibody is of molecular weight identical to that detected by a specific antiphospho-TrkB antibody directed against the phosphorylated form of the human peptide with the corresponding sequence [LQNLAKSPVT(PO3H2)LDIC; a gift from Dr. M. Chao; Iwakura et al., 2008], is also coimmunoprecipitated from *Xenopus* brain by the antiphospho-TrkB antibody (see Supp. Info. Fig. 1), and corresponds to the predicted molecular weight by cross-linking (Cohen-Cory et al., 1996).

A mouse monoclonal antibody against green fluorescent protein (GFP; Invitrogen, Eugene, OR; catalog No. A11120, clone 3E6) was generated with GFP, purified directly from *A. victoria*, as the antigen. The antibody has been shown to recognize specifically GFP and also recognizes a number of GFP variants including YFP (product information sheet). To control for specificity of immunostaining, nontransfected *Xenopus* tadpoles were incubated with the GFP antibody and processed for preembedding immunostaining or fluorescence immunohistochemistry as described below, showing negative immunoreactivity in all cases.

The antibody 3A 10, a mouse monoclonal antibody raised against chick nervous tissue that recognizes a neurofilament-associated protein, was developed by Drs. T.M. Jessell and J. Dodd (Columbia University), and was obtained from the Developmental Studies Hybridoma Bank developed under the auspices of the NICHD and maintained by The University of Iowa Department of Biological Sciences. The 3A 10 monoclonal antibody was generated by first immunizing mice against ventral spinal cord and assorted nervous tissue, then fusing splenocytes to mouse myeloma cell. In the *Xenopus* visual system, the 3A 10 antibody has been shown to immunostain RGCs specifically and their axon terminals both in vivo and in vitro (Hocking et al., 2008; Manitt et al., 2009) and showed an immunostaining pattern in

sections of the stage 45 *Xenopus* tadpole spinal cord comparable to that reported by Gravagna et al. (2008).

A mouse monoclonal antibody that recognizes the synaptosomal-associated protein-25 (SNAP-25; Assay Designs, Ann Arbor, MI; catalog No. VAM-SV0012, clone SP12) was used to identify presynaptic sites in the *Xenopus* tectal neuropil. This antibody was raised against synaptic vesicle containing fractions immunoprecipitated from human brain homogenates using anti-human synaptophysin monoclonal antibodies and recognizes a 25-kDa band by Western blot analysis. This anti-SNAP-25 monoclonal antibody exhibited an immunostaining pattern in *Xenopus* tadpoles identical to the one observed after immunostaining with a rabbit polyclonal antibody raised against a synthetic peptide, amino acid residues 195 – 206 of mouse SNAP-25 conjugated to KLH (Assay Designs; catalog No. VAP-SV002), a sequence that is conserved in human, chicken, and goldfish SNAP-25.

A rabbit polyclonal antibody against the vesicle-associated membrane protein VAMP2 (synaptobrevin; Assay Designs; calatog No. VAS-SV006), raised against a highly conserved 21-residue synthetic peptide QAQVDEVVDIMRVNVDKVLER based on the rat VAMP2 sequence (residues 36 – 56), recognizes human, mouse, rat, bovine, hamster, pig, and *Xenopus* VAMP2 (product information sheet) and was used to identify synaptic layers in the *Xenopus* tectal neuropil. In the *Xenopus* tadpole brain, VAMP2 immunoreactivity was confined to the well-defined synaptic layers, in a pattern identical to that found with antibodies to SNAP-25 and other synaptic vesicle proteins (Alsina et al., 2001; Manitt et al., 2009; Pinches and Cline, 1998).

Preembedding immunoelectron microscopy

Tadpoles with only a few RGCs expressing YFP in their axon terminals were selected and processed for preembedding immunoelectron microscopy. Tadpoles were anesthetized and fixed in 2% paraformaldehyde, 3.75% acrolein in 0.1 μM phosphate buffer, pH 7.4 (PB). Brains were removed, postfixed, and embedded in 1% agarose. Fifty-micrometer Vibratome sections were collected, incubated in 1% sodium borohydride in PB to block excess aldehyde groups, dipped in cryoprotectant (25% sucrose and 3.5% glycerol in 0.05 M PB, pH 7.4), quickly permeabilized in liquid nitrogen, and blocked in 0.5% bovine serum albumin (BSA), 0.1 M Tris-buffered saline (TBS), pH 7.5, for anti-GFP or 2% BSA for anti-TrkB immunostaining. Sections were incubated for 48 hours in a primary mouse monoclonal antibody against GFP (1:10 dilution in 0.1% BSA in TBS) or primary rabbit polyclonal antibody against *Xenopus* TrkB (1:2,000 in 0.5% BSA in TBS; custom-made antibody; Bethyl Labs) first at room temperature overnight and then at 4°C. For GFP immunostaining, sections were incubated in a secondary goat anti-mouse IgG coupled to 1-nm gold particles for 2 hours at RT (1:50 dilution in 0.5% v/v of 20% fish gelatin, 0.8% BSA in 0.01 M PBS, pH 7.4; Aurion-EMS, Hatfield, PA) and then incubated in 2% glutaraldehyde, and gold particles were enlarged using a British BioCell silver intensification kit (Ted Pella, Redding, CA). The high specificity but low sensitivity of this preembedding immunostaining technique resulted in discrete silver precipitates in immunopositive axon terminals (Rodriguez et al., 2005), which were absent in adjacent sections processed in the same manner but with the primary antibody omitted in the incubation bath. For TrkB immunostaining, sections were treated as described above but incubated for 2 hours in secondary biotinylated goat anti-rabbit IgG in 1.5% normal goat serum in 0.1 M PB, pH 7.4 and then transferred to an avidin/biotin/peroxidase solution (Vectastain Elite ABC kit; Vector Laboratories, Burlingame, CA; diluted 1:50 A and 1:50 B in 0.1 M PB, pH 7.4) for 1 hour in the dark at room temperature. Tissue was rinsed in 0.1 M PB, pH 7.4 and 0.1 M TBS, pH 7.5, sequentially, and then incubated in 0.022% diaminobenzidine (DAB kit; Sigma, St. Louis, MO) in 0.003% hydrogen peroxide in TBS for 2 minutes at room temperature to visualize the immunostaining. The reaction was stopped by dipping the

sections in 0.1 M TBS, pH 7.5. As controls for specificity of immunostaining, sections adjacent to those incubated with GFP or TrkB antibodies were incubated without primary or secondary antibodies.

Electron microscopy

Sections were postfixed in 2% osmium tetroxide, dehydrated, and flat embedded in 100% Epon between Aclar sheets (Ted Pella, Inc.). With the use of a stereoscope, the optic tectum was carefully dissected and placed on Epon blocks. Blocks were coded, and all subsequent procedures were performed blind to treatment groups. Seventy-nanometer thin sections were obtained on copper mesh grids using a Reichert ultramicrotome with a diamond knife (Diatome, Biel, Switzerland) and counterstained with 2% uranyl acetate and Reynolds lead citrate. In a number of samples not used for immunostaining, brains were embedded in LR-white (Ted Pella, Inc.). Ultrastructural analysis was performed using a Philips (Aachen, Germany) CM10 transmission electron microscope. Electron micrographs were captured at ×6.6 – 8.9K magnifications using a Bio-Scan CCDTV (Gatan Inc., Pleasanton, CA) and were saved as high-resolution TIFF files (2,048 × 2,048 pixels). Digital images were optimized for image resolution (final resolution 350 dpi), brightness, and contrast in Photoshop CS2 (Adobe Systems, San Jose, CA). Pre- and postsynaptic terminals were highlighted in the adjusted and cropped images by coloring background layers at 25% opacity in Photoshop CS2.

Ultrastructural analysis

Synapses were identified by the thickening of the pre- and postsynaptic membranes and the presence of vesicles in close proximity to the presynaptic zone. Some synaptic terminals exhibited multiple synaptic profiles, and synaptic profiles were defined as a single presynaptic element containing at least three synaptic vesicles apposed to a postsynaptic element with membrane specialization. For quantitative analysis, the number of synaptic vesicles within the presynaptic terminal area at mature synapses (synapses with well-defined pre- and postsynaptic densities) and the number of docked vesicles per terminal (attached to the presynaptic density at a distance less than 50 nm) were measured. The length of the presynaptic specialization and the size of the area of the axon terminal were measured in ImageJ (W.S. Rasband, U.S. National Institutes of Health; http://rsb.info.nih.gov/ij/, 1997 – 2005).

Four sections per brain from stage 45 control tadpoles (n = 11 tadpoles), tadpoles treated with BDNF and killed 24 hours postinjection (n = 9 tadpoles), and tadpoles treated with BDNF and killed at 8 hours (n = 7 tadpoles) were analyzed. For the analysis of changes in synapse number elicited by BDNF, the number of YFP-positive synaptic profiles was normalized to the total number of YFP-positive profiles encountered within the tectal neuropil for each brain and then averaged for all brains from each individual treatment. One-way ANOVA and two-sample unpaired Student *t*-tests were used for the statistical analysis of data. Significance was set at $P < 0.05$.

Immunohistochemistry

For immunohistochemistry colocalization studies, the affinity-purified rabbit polyclonal antibody against *Xenopus* TrkB, a mouse monoclonal antibody that recognizes a neurofilament-associated protein (3A 10 antibody), and a mouse monoclonal antibody to SNAP-25 were used (see above and Table 1). Tadpoles were anesthetized and fixed by immersion in 2% paraformaldehyde and 3.75% acrolein in 0.1 M phosphate buffer pH 7.4 (PB); the brains were removed and postfixed with the same fixative for 1 hour. Horizontal free-floating vibratome sections (25 μm) were obtained, preincubated in blocking solution (2% BSA, 0.1% Triton X-100 in 0.1 M PB), and incubated overnight with anti-TrkB (rabbit

IgG; 1:2,000) and anti-SNAP-25 (mouse IgG, 1:1,000) or anti-TrkB and 3A 10 antibody (mouse IgG, 1:2,000). A rabbit polyclonal antibody against VAMP2 was used at a 1:1,000 dilution in 2% BSA 0.1% Triton X-100 in 0.1 MPB to delineate the synaptic layer within the neuropil of the tadpole optic tectum (see Fig. 1). For endogenous TrkB and 3A 10 colocalization in the retina, stage 45 tadpoles were fixed in 4% paraformaldehyde; 20-μm cryostat sections were obtained and incubated with anti-TrkB (rabbit IgG, 1:2,000) and 3A 10 antibody (mouse IgG, 1:2,000). Tissues were then rinsed and incubated with Alexa 488 anti-rabbit and Alexa 568 anti-mouse antibodies (1:200 dilution each in 0.1 M PB; Invitrogen, Eugene, OR). All images were collected with a LSM 5 Pascal confocal microscope (Zeiss, Jena, Germany) using a ×63/1.4 NA oil immersion objective. To determine colocalization of fluorescent labels, optical sections were collected at 0.5-μm intervals. When appropriate, confocal stacks were projected into one plane using the LSM 5 Image Browser software (Zeiss) and converted into TIFF files. Digital images were optimized for resolution (final resolution 300 dpi) without contrast or gain enhancements in Photoshop CS2, prior to creating individual figure montages.

RESULTS

Ultrastructural characterization of the synaptic connectivity in the *Xenopus* optic tectum was obtained at two stages of development; stage 40, when RGC axons begin to innervate the optic tectum and when synaptic activity is first recorded (Tao et al., 2001; Zhang et al., 1998), and stage 45, when RGC axons are actively branching and making synapses with postsynaptic tectal neurons (Alsina et al., 2001). In *Xenopus*, RGC axons project contralaterally to their target, the optic tectum, and make connections with dendrites of postsynaptic neurons in the tectal neuropil. The tectal neuropil is located in the lateral portion of the midbrain and is devoid of cell bodies but is rich in dendrites and axonal processes originating from afferent/projecting neurons as well as interneurons (Fig. 1A,B). Thus, to identify specifically retinotectal synapses within the tectal neuropil, RGCs were transfected with YFP in young embryos, and the afferent RGC axons expressing YFP and terminating in the optic tectum were identified by preembedding immunohistochemistry (Fig. 1C). Ultrastructural analysis of the tectal neuropil of stage 40 *Xenopus* tadpoles showed significant extracellular space between axonal and dendritic profiles (Fig. 2A), with the neuropil being less dense than in more mature synaptic circuits, similar to the ultrastructural organization of the optic tectum of *Rana pipiens* larvae (Norden and Constantine-Paton, 1994; Reh and Constantine-Paton, 1984). At this developmental stage, numerous axonal and dendritic filopodia-like profiles were observed (Fig. 2A – C). Filopodial profiles were categorized as such and differentiated from mature dendrites and axons by their usually narrow, cylindrical shape; their pointy tips; and their dense, granular cytoplasm rich in actin (Markham and Fifkova, 1986; Skoff and Hamburger, 1974). Axonal filopodia-like profiles were clearly distinguished from their dendritic counterparts by the presence of synaptic vesicles and were observed to make synaptic contact with adjacent dendritic filopodia-like profiles (Fig. 2B,C), similarly to the early forms of synaptic contact in embryonic mouse spinal cord (Vaughn, 1989). Nascent asymmetric synapses between YFP-identified RGC axonal profiles and postsynaptic profiles were observed at this stage (Fig. 2B,C), although a significant portion of the axonal profiles was also nonsynaptic (approximately 55%; data not shown). In some cases, axonal and dendritic profiles were multisynaptic, establishing more than one synaptic contact along their length (Fig. 2C). The presence of multisynaptic contacts on axonal and dendritic filopodia-like profiles is in agreement with the early synaptic ultrastructural organization of the mammalian hippocampus and spinal cord (Fiala et al., 1998; Vaughn, 1989). No synaptic profiles on dendritic shafts or spines were observed in the stage 40 *Xenopus* tectal neuropil, supporting the idea that filopodially mediated interactions between axonal terminals and dendritic processes mediate early synaptogenesis in the developing tadpole at this stage (Cohen-Cory,

2002; Jontes et al., 2000; Jontes and Smith, 2000; Lohmann and Bonhoeffer, 2008; see Discussion). Astrocytes, distinguished from neurons by the presence of gliofilaments, glycogen granules, rather clear cytoplasm, and irregular stellate shape (Peters et al., 1991), were seldom observed in the tectal neuropil at this stage, an observation corroborated by the absence of staining when using conventional glial markers (C. Manitt, S. Chakravarthy, and S. Cohen-Cory, unpublished observations).

Ultrastructural organization of the stage 45 *Xenopus* optic tectal neuropil

Significant changes were observed in the ultrastructural synaptic organization of the *Xenopus* optic tectum as embryos grow and mature (Figs. 2, 3). At stage 45 (approximately 48 hours of further differentiation past stage 40), the midbrain optic tectum appeared more mature and compact, with a larger portion of the tissue forming the tectal neuropil (not shown). Neuronal cell bodies in the optic tectum continue to differentiate and localize to the more medial portion of the brain, near the ventricle, and project their primary dendrites laterally to the tectal neuropil (Fig. 1A, diagram). The *Xenopus* tectal neuropil at this stage is characterized by the abundance of mitochondria and the presence of mature synapses (Figs. 3B,C, 4, 6) as well as synapses on filopodia-like profiles (Fig. 5). No myelinating glia or myelinated processes were observed at this stage. Mature asymmetric synapses were identified as those that had a presynaptic terminal with at least three synaptic vesicles near the presynaptic zone and directly apposed to a postsynaptic terminal with a well-defined postsynaptic density (PSD; see Fig. 3B,C as examples).Two distinct types of synaptic vesicles were identified in synapses in the stage 45 tectal neuropil; the most common were small, clear, and round (Fig. 3C; see also Figs. 4 – 7), typically described as containing classical neurotransmitters (Peters et al., 1991), and a second type and less abundant were dense-core vesicles (Fig. 3D), usually associated with neuropeptide storage and secretion (Peters et al., 1991). Dendritic (Fig. 3D) and axonal (not shown) profiles containing multivesicular bodies were also observed at this stage.

As for the stage 40 tadpoles, we identified retinotectal synapses in stage 45 *Xenopus* tadpoles by the specific expression and anterograde transport of YFP in RGCs. The majority of retinotectal synapses at this stage were axodendritic, in which a mature dendritic profile received input from a YFP-identified axon terminal (Figs. 4, 6A,B; see also Table 2). Most of the axodendritic synapses identified were shaft synapses (40.3% ± 6.8% of 104 synaptic profiles from a total of 11 brains), where the axon profile made clear contact with a dendrite shaft. Retinal axon terminals were also observed to make contact with dendritic protrusions that resemble spines (Fig. 4). Most dendritic spine-like profiles were monosynaptic, receiving a single contact from an axon terminal (Fig. 4A,C,D), although spine-like profiles that received more than one synaptic contact were also observed (Fig. 4B). Although the existence of dendritic spines in the *Xenopus* tectal neuropil has remained elusive at this stage, our results clearly demonstrate that a significant number of retinotectal synapses are made on dendritic protrusions that resemble spines (8.5% ± 4.5%; see Figs. 3C, 4; see also Supp. Info. Fig. 2). These spiny protrusions present in some tectal neurons in the developing *Xenopus* tadpole differ from those commonly observed in mammalian hippocampus and cortical neurons, in that they are smaller and less abundant (Supp. Info. Fig. 2). Thus, our observations indicate that mature synaptic structures that resemble those of higher vertebrate systems are present in developing brain of *Xenopus* tadpoles at this stage. Immature dendritic profiles with filopodia-like processes receiving input from RGC axon terminals were still observed in the tectal neuropil at stage 45 (Fig. 5C,D). However, the overall density of filopodia-like synaptic profiles was reduced relative to that in the stage 40 brain. Less than half of the total retinotectal synapses identified at stage 45 were on filopodia-like dendritic profiles (47.5% ± 6.7%), in agreement with in vivo observations of ongoing dynamic synaptogenesis in this system at this stage (Alsina et al., 2001;Ruthazer et al.,

2006). A small portion of axodendritic synapses observed resembled perforated synapses (4.86% ± 2.5%), synapses that are characterized by a split postsynaptic density (Calverley and Jones, 1990), and these occurred mostly on dendritic shafts (not shown). Although infrequent, axoaxonal synapses were also observed in the stage 45 tadpole brain (Fig. 6C,D). Only about 3% (3.5% ± 1.8%) of the total retinotectal synapses characterized in our analysis were axoaxonal at this stage.

BDNF alters the ultrastructural composition of synapses

Previous studies from our laboratory have shown that BDNF enhances branching and complexity of *Xenopus* RGC axonal arbors (Cohen-Cory and Fraser, 1995), increases presynaptic site differentiation (Alsina et al., 2001), and stabilizes presynaptic sites and axon branches (Hu et al., 2005). To determine the relationship between the effects of BDNF on presynaptic site formation and the synaptic maturation of RGC axon arbors, we then examined the effects of BDNF treatment on the ultrastructure of YFP-identified retinotectal synapses. BDNF was injected in the optic tectum of stage 45 tadpoles with RGC expressing YFP, and animals were killed 8 and 24 hours after treatment. Control tadpoles, from the same spawning, with RGC axons expressing YFP were similarly microinjected with vehicle solution at stage 45 and killed 8 and 24 hours postinjection. No significant differences were observed in the ultrastructural characteristics of the two control groups (data not shown); therefore, these two groups were combined for statistical analysis of data.

Several parameters were measured in samples of tadpole brains to examine potential acute effects of BDNF on retinotectal synapses. The relative number of synaptic profiles identified in control and BDNF-treated optic tectum was determined to obtain a measure of overall synaptic changes elicited by BDNF. Twenty-four hours after BDNF injection, the number of YFP-positive synaptic profiles was significantly higher in the BDNF-treated tectal neuropil than in controls (BDNF 60.25% ± 3.9%, control 46.3% ± 4.2%; $P = 0.049$; see Materials and Methods). However, there was no significant difference in the number of synaptic profiles identified 8 hours after BDNF treatment compared with controls (40.43% ± 4.35%; $P > 0.05$). To determine whether the BDNF treatment altered the relative proportion or distribution of synapses, we classified the YFP-identified retinotectal synapses present in the tectal neuropil of tadpoles 8 and 24 hours after BDNF treatment. A significant increase in the relative proportion of synapses on spine-like profiles was observed in tadpoles 24 hours after BDNF treatment compared with controls (control 8.5% ± 4.56%, n = 104 synaptic profiles from 11 tadpoles; BDNF 29% ± 4.63%, n = 101 profiles from 9 tadpoles; Table 2). High variability in the number of synapses on spine-like profiles was observed 8 hours after BDNF treatment (24.9% ± 13.14%, n = 79 synaptic profiles, seven tadpoles), with a trend toward an increase in their relative proportion, as seen at 24 hours. No other significant differences in the number of axoaxonal, filopodia-like, and axodendritic synapses were observed between controls and BDNF-treated tadpoles at 8 hours (not shown) or 24 hours (Table 2).

To examine further whether BDNF treatment alters the ultrastructural characteristics of retinotectal synapses, we measured the number and density of synaptic vesicles per profile ($N/\mu m^2$), the number of docked synaptic vesicles (N/μm), and the length of the active zone (postsynaptic density; in nm) in YFP-identified retinotectal synapses in controls and BDNF-treated tadpoles (Table 3). For this analysis, in total 80 YFP-identified retinotectal synaptic terminals were analyzed for controls, 69 for the BDNF treated group after 8 hours, and 71 for tadpoles killed 24 hours post-BDNF treatment. No significant difference in the total number or density of synaptic vesicles per profile was observed between controls and BDNF-treated tectum, either 8 or 24 hours after treatment (Table 3).

A relative measure of the effectiveness of synaptic transmission is the number of docked synaptic vesicles at the presynaptic active zone (Harris and Sultan, 1995; Schikorski and Stevens, 1997; Tyler and Pozzo-Miller, 2001). We observed that the number of docked synaptic vesicles was similar in the control tadpole tectal neuropil and in tadpoles microinjected with BDNF 8 hours after treatment (control 6.46 ± 0.47 vesicles, BDNF 8 hours 7.42 ± 0.57). The density of docked vesicles, however, was significantly lower in the BDNF tadpoles 8 hours after treatment compared with controls (BDNF 8 hours 27.92 ± 3.68 vesicles/μm, control 39.17 ± 3.68 vesicles/μm; $P = 0.012$), and this seemed to result from an increase in the length of the active zone (BDNF 8 hours 290 ± 19 nm, controls 206 ± 10 μm; $P < 0.0001$; Fig. 7A,B). Although the total number of docked vesicles was not altered 8 hours after BDNF treatment, we observed that by 24 hours there was a significant increase in docked vesicle number compared with controls (BDNF 24 hours, 8.15 ± 0.52 docked vesicles, controls 6.46 ± 0.47 docked vesicles; $P = 0.0162$; Table 3; Fig. 7). The length of the active zone (225 ± 12 nm) and the overall density of docked vesicles per active zone (39.97 ± 2.43 vesicles/μm), however, were not significantly different from controls 24 hours after BDNF treatment. Thus, the BDNF-elicited effect on synapse size (active zone) observed 8 hours after treatment appeared to be transient.

No differences in the relative proportion of RGC axonal profiles making multisynaptic contacts were observed in the neuropil of control or BDNF-treated tadpoles. For control tadpoles, 15.7% ± 4.6% of all YFP-identified synaptic profiles were multisynaptic, whereas 8.33% ± 3.66% were multisynaptic 24 hours post-BDNF injection ($P = 0.183$). A slight difference in the type of postsynaptic targets of multisynaptic profiles was observed, however, between controls and BDNF-treated tadpoles at 8 and 24 hours. For controls, close to 50% of the multisynaptic contacts were on immature, filopodia-like profiles; 38.46% were on dendritic profiles; and 3.85% were on protrusions that resemble spines (spine-like profiles). In contrast, 8 hours after BDNF administration, only 20% of the multisynaptic contacts occurred on filopodia-like profiles, 40% on dendrites, and 20% on spine-like profiles. Twenty-four hours after BDNF treatment, 50% of the YFP-identified RGC multisynaptic contacts were on dendrites and 31.25% on spine-like profiles, whereas only 12.5% were on filopodia-like profiles. These observations suggest a gradual, BDNF-elicited shift in multisynaptic RGC axon contacts from filopodia to dendrites and spines.

TrkB is expressed both pre- and postsynaptically in the *Xenopus* optic tectum

Studies from our laboratory have demonstrated that BDNF, signaling through its receptor TrkB (Soppet et al., 1991; Squinto et al., 1991), influences the synaptic connectivity of developing RGCs with tectal neurons by acting presynaptically (Hu et al., 2005; Marshak et al., 2007; Sanchez et al., 2006). Specifically, manipulating TrkB signaling by overexpression of a truncated form of the receptor in single presynaptic RGCs altered RGC axon arbor morphology and synaptic connectivity, whereas similar manipulation of postsynaptic tectal neurons did not affect tectal neuron dendritic morphology or connectivity (Marshak et al., 2007). These results raised the possibility that, in the retinotectal system, TrkB functions exclusively presynaptically and that this may be due to the specific localization of the TrkB receptor to RGC axon terminals. To explore this possibility directly, we generated an antibody against the intracellular domain of the *Xenopus* TrkB receptor (see Materials and Methods and Supp. Info. Fig. 1). Immunohistochemical studies demonstrate that TrkB is expressed in the retina, by RGCs (Supp. Info. Fig. 3; see also Cohen-Cory et al., 1996), and in the tectal neuropil where RGC axons project (Fig. 8; Supp. Info. Fig. 3). There is a high degree of colocalization of TrkB expression in the optic tectum with presynaptic markers (Fig. 8A – C). Immunostaining with the TrkB antibody shows, however, that TrkB is also associated with neurons in the optic tectum that are in close proximity to the neuropil (Fig. 8B), suggestive of TrkB-positive terminals contacting differentiated neurons and/or

endogenous expression by a subset of tectal neurons. To differentiate between these possibilities further, we performed immunoelectron microscopy studies to determine the subcellular distribution of TrkB. Our studies reveal that full-length TrkB is expressed both presynaptically (on axon terminals) and postsynaptically (on dendrites) in the tectal neuropil (Fig. 8D,E), with similar frequency (about 42.5% of immunoreactive profiles were axon terminals, and 54.8% were dendrites, n = 42 terminals identified from three brains and three sections per brain). In presynaptic terminals, TrkB immunoreactivity was localized near the synapse and was associated with synaptic vesicles, an observation that is in agreement with observations made in mammalian hippocampal neurons (Drake et al., 1999). Conversely, when localized postsynaptically, immunolabeling was observed in close proximity to the postsynaptic density, indicating that the TrkB receptor can be both pre- and postsynaptic in this system.

DISCUSSION

Here we provide an ultrastructural characterization of the developing retinotectal circuit of *Xenopus laevis*. Our electron microscopy studies of identified retinotectal synapses show that there is a significant synaptic maturation in this circuit over a relatively short period of time. The synaptic circuit within the tectal neuropil transitions rapidly from a relatively immature state, when retinotectal synapses are formed mainly on developing filopodia-like processes, to a more mature state, when mature synapses are established between RGC axon terminals and dendritic spines and shafts. This transition takes place from stage 40 to stage 45 (within 2 – 3 days) and coincides morphologically with a period of active axon and dendritic remodeling (Cline, 2001; Cohen-Cory and Fraser, 1995; O'Rourke and Fraser, 1990; Tao and Poo, 2005). Physiologically, these structural changes at synapses coincide with the period when visually evoked synaptic inputs refine and become precise in the retinotectal system (Tao and Poo, 2001).

Imaging studies in culture systems have shown that early interactions between axon and dendritic filopodia seem to underlie the selection of potential synaptic partners before a functional synapse is formed (Tashiro et al., 2003; Ziv and Smith, 1996), and these interactions involve communication through nonsynaptic calcium transients (Lohmann and Bonhoeffer, 2008). Imaging studies in vivo support the notion that transient synapses may be formed and dismantled as axons and dendrites remodel (Alsina et al., 2001; Meyer and Smith, 2006; Ruthazer et al., 2006). Our ultrastructural studies demonstrate early interactions between dendritic and axonal filopodia-like processes prior to and during the peak period of synaptogenesis in the *Xenopus* retinotectal system and thus support the active involvement of these structures in selecting the correct partners in the developing intact brain (Tashiro et al., 2003). These observations are also in agreement with studies in chick and mammals, in which dendritic growth cones and filopodia bear synapses during active synaptogenesis (Fiala et al., 1998; Skoff and Hamburger, 1974). Our studies also reveal a period of transition from more immature synaptic contacts to the establishment of asymmetric (excitatory) synapses by RGC axon terminals on shafts as well as dendritic spines of tectal neurons. The existence of spine synapses in the developing *Xenopus* retinotectal system is a novel finding, insofar as spine structures can seldom be discerned on neurons labeled with fluorescent tracers in this species (however, see Supp. Info. Fig. 2 and Rybicka and Udin, 1994). The occurrence of primarily filopodia-like, then shaft, and then spine-like synapses during retinotectal development is also in agreement with observations that filopodia recruit shaft synapses that later give rise to spines in mammals (Fiala et al., 1998).

Effects of BDNF on synapse ultrastructure

In previous studies we used targeted, acute alterations in BDNF levels within the tadpole optic tectum to demonstrate that BDNF influences the establishment of synaptic connectivity between RGC axons and tectal neurons, primarily by influencing RGCs (Alsina et al., 2001; Hu et al., 2005; Sanchez et al., 2006). Direct manipulations of TrkB signaling in individual RGCs have also confirmed that BDNF acts on RGC axons to alter their synaptic connectivity (Marshak et al., 2007). Specifically, axons from RGCs overexpressing a dominant negative form of the TrkB receptor establish fewer synapses with tectal neurons, and synapse ultrastructure in those axons is also altered. Thus, as a result of chronically interfering with presynaptic TrkB signaling, presynaptic sites in RGC axons contain fewer synaptic vesicles overall, and the number of synaptic vesicles docked at active zones is also decreased (Marshak et al., 2007). The effects of acute treatment with BDNF on synaptic ultrastructure observed here, though milder, are in agreement with our previous observations, insofar as docked synaptic vesicle number is significantly increased 24 hours after BDNF treatment. The difference in the effect of BDNF treatment vs. overexpression of dominant negative TrkB on RGCs may therefore be due to acute vs. chronic changes caused by each of these manipulations and/or by possible differences in the site of action by BDNF (see below).

Similarly to our findings, BDNF treatment increases the number of vesicles docked at active zones in the chick optic tectum (Wang et al., 2003) and at excitatory synapses in rat hippocampus (Tyler and Pozzo-Miller, 2001; Tyler et al., 2006). Consistent with an effect on a modulatory role of BDNF in synaptic function are observations that the number of docked vesicles is reduced at hippocampal synapses in BDNF knockout mice (Pozzo-Miller et al., 1999) and that deficits in TrkB signaling result in down-regulation of neurotransmitter release at synaptic sites and decreased expression of synaptic proteins responsible for synaptic vesicle docking and fusion (Lin and Scheller, 2000; Martinez et al., 1998; Otal et al., 2005). Neurotransmitter release probability is proportional to the number of docked synaptic vesicles (Pozzo-Miller et al., 1999; Schikorski and Stevens, 2001; Tyler and Pozzo-Miller, 2001), so the structural changes at the level of individual synapses that we observed reflect the ability of BDNF to alter synaptic function. These ultrastructural changes observed at individual synapses are also consistent with electrophysiological studies showing persistent potentiation of retinotectal synapses in tadpoles with acute increases in BDNF tectal levels (Du and Poo, 2004).

Our ultrastructural studies also demonstrate that BDNF treatment increases the proportion of retinotectal synapses formed on spine-like protrusions within 24 hours following treatment. Previous imaging studies from our laboratory showed that acute treatment with BDNF increases postsynaptic site differentiation on tectal neurons (number of PSD-95 – GFP-labeled postsynaptic sites), but this event is delayed when contrasted to the effects of BDNF on presynaptic sites on RGC axons (Sanchez et al., 2006). These observations and additional manipulations in TrkB signaling in tectal neurons (Marshak et al., 2007) led to the interpretation that the effects of BDNF on postsynaptic neurons are secondary to those on RGC axons. A protracted effect of BDNF on spine synaptogenesis is in agreement with observations made in hippocampal neurons in culture, in which mature spine synapses are formed within 10 – 15 hours of initial contact by a nascent spine at presynaptic buttons (Nagerl et al., 2007). Thus, the increase in spine-like synapses elicited by BDNF may also reflect a transition from an early synaptic contact that involves the accumulation of pre- and postsynaptic components at nascent synaptic sites, to the later maturation of a synapse. The observation of a transient increase in length of the active zone 8 hours after BDNF treatment also supports the existence of gradual synaptic rearrangements that can serve to maximize synaptic strength: BDNF may possibly influence the readily releasable synaptic vesicle pool by first inducing an enlargement of the active zone (Wittig and Parsons, 2008) and then

increasing the number of docked synaptic vesicle at the active zone (Tyler and Pozzo-Miller, 2001). In the mammalian brain, BDNF has been shown to play a role in de novo spine formation, spine dynamics, and the sculpting of existing dendritic spines (Alonso et al., 2004; Horch et al., 1999; Tyler and Pozzo-Miller, 2001, 2003), so it is possible that the BDNF-elicited shift in the relative proportion of *Xenopus* retinotectal synapses that are made on spine-like processes may indeed reflect effects on synapse formation and maturation rather than retargeting of existing synapses. Changes in the structure of dendritic spines involve active remodeling of the actin cytoskeleton, and BDNF can modulate this process (for review see Amaral et al., 2007; Bramham, 2008; Yuste and Bonhoeffer, 2001). High-resolution in vivo imaging followed by retrospective serial electron microscopy at the level of single axons and/or dendritic branches (as in Yen et al., 1993), however, would be necessary to provide a definitive dynamic mechanism by which BDNF affects the fine structure of retinotectal synapses.

Our studies demonstrating the expression of TrkB at pre- and postsynaptic sites indicate that TrkB-mediated BDNF signaling participates actively in synapse formation and stabilization but do not distinguish the site of action of BDNF. Characterization studies in several neuronal systems and species indicate that TrkB localizes to axon terminals and functions presynaptically (Drake et al., 1999; Gomes et al., 2006; Swanwick et al., 2004). Studies have also suggested that BDNF may only act postsynaptically, insofar as TrkB is absent from axon terminals and growth cones in some systems (Elmariah et al., 2004). The expression of TrkB on dendrites of neurons in cortex, hippocampus, and many other neuronal circuits (Aoki et al., 2000; Drake et al., 1999; Gomes et al., 2006; Swanwick et al., 2004) supports both pre- and postsynaptic actions by BDNF. Although all of our studies in which BDNF levels and TrkB expression have been experimentally manipulated support a presynaptic action by BDNF on RGC presynaptic differentiation and axon branching (Marshak et al., 2007; Sanchez et al., 2006), we cannot exclude the possibility that BDNF may also exert some effects on postsynaptic tectal neurons, because our current immunohistochemical and immunoelectron microscopy studies reveal that TrkB is expressed both pre- and postsynaptically in this circuit. It is possible, thus, that BDNF may affect aspects of tectal neuron function that are independent of the effects of BDNF on presynaptic axon terminals and that these effects were not revealed by our previous in vivo imaging studies. Potential postsynaptic actions of BDNF in the *Xenopus* retinotectal circuit therefore deserve further investigation.

Supplementary Material

Refer to Web version on PubMed Central for supplementary material.

Acknowledgments

We thank Tiffany Nguyen, Blanca Morales, Nicole Shirkey, and Ymkje Anna de Vries for help with some aspects of this work; Dr. Charles Ribak for access to the electron microscopy unit; and members of our laboratory for helpful comments on the manuscript.

Grant sponsor: National Eye Institute; Grant number: EY011912.

LITERATURE CITED

Alonso M, Medina JH, Pozzo-Miller L. ERK1/2 activation is necessary for BDNF to increase dendritic spine density in hippocampal CA 1 pyramidal neurons. Learn Mem 2004;11:172–178. [PubMed: 15054132]

Alsina B, Vu T, Cohen-Cory S. Visualizing synapse formation in arborizing optic axons in vivo: dynamics and modulation by BDNF. Nat Neurosci 2001;4:1093–1101. [PubMed: 11593233]

Amaral MD, Chapleau CA, Pozzo-Miller L. Transient receptor potential channels as novel effectors of brain-derived neurotrophic factor signaling: potential implications for Rett syndrome. Pharmacol Ther 2007;113:394–409. [PubMed: 17118456]

Aoki C, Wu K, Elste A, Len G, Lin S, McAuliffe G, Black IB. Localization of brain-derived neurotrophic factor and TrkB receptors to postsynaptic densities of adult rat cerebral cortex. J Neurosci Res 2000;59:454–463. [PubMed: 10679783]

Bramham CR. Local protein synthesis, actin dynamics, and LTP consolidation. Curr Opin Neurobiol 2008;18:524–531. [PubMed: 18834940]

Calverley RK, Jones DG. Contributions of dendritic spines and perforated synapses to synaptic plasticity. Brain Res Brain Res Rev 1990;15:215–249. [PubMed: 2289086]

Cline HT. Dendritic arbor development and synaptogenesis. Curr Opin Neurobiol 2001;11:118–126. [PubMed: 11179881]

Cohen-Cory S. The developing synapse: construction and modulation of synaptic structures and circuits. Science 2002;298:770–776. [PubMed: 12399577]

Cohen-Cory S, Fraser SE. Effects of brain-derived neurotrophic factor on optic axon branching and remodelling in vivo. Nature 1995;378:192–196. [PubMed: 7477323]

Cohen-Cory S, Lom B. Neurotrophic regulation of retinal ganglion cell synaptic connectivity: from axons and dendrites to synapses. Int J Dev Biol 2004;48:947–956. [PubMed: 15558485]

Cohen-Cory S, Escandon E, Fraser SE. The cellular patterns of BDNF and trkB expression suggest multiple roles for BDNF during *Xenopus* visual system development. Dev Biol 1996;179:102–115. [PubMed: 8873757]

Drake CT, Milner TA, Patterson SL. Ultrastructural localization of full-length trkB immunoreactivity in rat hippocampus suggests multiple roles in modulating activity-dependent synaptic plasticity. J Neurosci 1999;19:8009–8026. [PubMed: 10479701]

Du JL, Poo MM. Rapid BDNF-induced retrograde synaptic modification in a developing retinotectal system. Nature 2004;429:878–883. [PubMed: 15215865]

Elmariah SB, Crumling MA, Parsons TD, Balice-Gordon RJ. Postsynaptic TrkB-mediated signaling modulates excitatory and inhibitory neurotransmitter receptor clustering at hippocampal synapses. J Neurosci 2004;24:2380–2393. [PubMed: 15014113]

Fiala JC, Feinberg M, Popov V, Harris KM. Synaptogenesis via dendritic filopodia in developing hippocampal area CA 1. J Neurosci 1998;18:8900–8911. [PubMed: 9786995]

Gomes RA, Hampton C, El-Sabeawy F, Sabo SL, McAllister AK. The dynamic distribution of TrkB receptors before, during, and after synapse formation between cortical neurons. J Neurosci 2006;26:11487–11500. [PubMed: 17079678]

Gravagna NG, Knoeckel CS, Taylor AD, Hultgren BA, Ribera AB. Localization of Kv2.2 protein in *Xenopus laevis* embryos and tadpoles. J Comp Neurol 2008;510:508–524. [PubMed: 18680201]

Harris KM, Sultan P. Variation in the number, location and size of synaptic vesicles provides an anatomical basis for the nonuniform probability of release at hippocampal CA 1 synapses. Neuropharmacology 1995;34:1387–1395. [PubMed: 8606788]

Hocking JC, Hehr CL, Chang RY, Johnston J, McFarlane S. TGFbeta ligands promote the initiation of retinal ganglion cell dendrites in vitro and in vivo. Mol Cell Neurosci 2008;37:247–260. [PubMed: 17997109]

Horch HW, Kruttgen A, Portbury SD, Katz LC. Destabilization of cortical dendrites and spines by BDNF. Neuron 1999;23:353–364. [PubMed: 10399940]

Hu B, Nikolakopoulou AM, Cohen-Cory S. BDNF stabilizes synapses and maintains the structural complexity of optic axons in vivo. Development 2005;132:4285–4298. [PubMed: 16141221]

Hua JY, Smith SJ. Neural activity and the dynamics of central nervous system development. Nat Neurosci 2004;7:327–332. [PubMed: 15048120]

Iwakura Y, Nawa H, Sora I, Chao MV. Dopamine D1 receptor-induced signaling through TrkB receptors in striatal neurons. J Biol Chem 2008;283:15799–15806. [PubMed: 18381284]

Jontes JD, Smith SJ. Filopodia, spines, and the generation of synaptic diversity. Neuron 2000;27:11–14. [PubMed: 10939326]

Jontes JD, Buchanan J, Smith SJ. Growth cone and dendrite dynamics in zebrafish embryos: early events in synaptogenesis imaged in vivo. Nat Neurosci 2000;3:231–237. [PubMed: 10700254]

Lin RC, Scheller RH. Mechanisms of synaptic vesicle exocytosis. Annu Rev Cell Dev Biol 2000;16:19–49. [PubMed: 11031229]

Lohmann C, Bonhoeffer T. A role for local calcium signaling in rapid synaptic partner selection by dendritic filopodia. Neuron 2008;59:253–260. [PubMed: 18667153]

Luikart BW, Parada LF. Receptor tyrosine kinase B-mediated excitatory synaptogenesis. Prog Brain Res 2006;157:15–24. [PubMed: 17167900]

Manitt C, Nikolakopoulou AM, Almario DR, Nguyen SA, Cohen-Cory S. Netrin participates in the development of retinotectal synaptic connectivity by modulating axon arborization and synapse formation in the developing brain. J Neurosci 2009;29:11065–11077. [PubMed: 19741113]

Markham JA, Fifkova E. Actin filament organization within dendrites and dendritic spines during development. Brain Res 1986;392:263–269. [PubMed: 3708380]

Marshak S, Nikolakopoulou AM, Dirks R, Martens GJ, Cohen-Cory S. Cell autonomous TrkB signaling in presynaptic retinal ganglion cells mediates axon arbor growth and synapse maturation during the establishment of retinotectal synaptic connectivity. J Neurosci 2007;27:2444–2456. [PubMed: 17344382]

Martinez A, Alcantara S, Borrell V, Del Rio JA, Blasi J, Otal R, Campos N, Boronat A, Barbacid M, Silos-Santiago I, Soriano E. TrkB and TrkC signaling are required for maturation and synaptogenesis of hippocampal connections. J Neurosci 1998;18:7336–7350. [PubMed: 9736654]

Meyer MP, Smith SJ. Evidence from in vivo imaging that synaptogenesis guides the growth and branching of axonal arbors by two distinct mechanisms. J Neurosci 2006;26:3604–3614. [PubMed: 16571769]

Mumm JS, Williams PR, Godinho L, Koerber A, Pittman AJ, Roeser T, Chien CB, Baier H, Wong RO. In vivo imaging reveals dendritic targeting of laminated afferents by zebrafish retinal ganglion cells. Neuron 2006;52:609–621. [PubMed: 17114046]

Nagerl UV, Kostinger G, Anderson JC, Martin KA, Bonhoeffer T. Protracted synaptogenesis after activity-dependent spinogenesis in hippocampal neurons. J Neurosci 2007;27:8149–8156. [PubMed: 17652605]

Niell CM, Meyer MP, Smith SJ. In vivo imaging of synapse formation on a growing dendritic arbor. Nat Neurosci 2004;7:254–260. [PubMed: 14758365]

Nieuwkoop, PD.; Faber, J. Normal table of *Xenopus laevis*. Amsterdam: Elsevier North Holland; 1956.

Norden JJ, Constantine-Paton M. Dynamics of retinotectal synaptogenesis in normal and 3-eyed frogs: evidence for the postsynaptic regulation of synapse number. J Comp Neurol 1994;348:461–479. [PubMed: 7844258]

O'Rourke NA, Fraser SE. Dynamic changes in optic fiber terminal arbors lead to retinotopic map formation: an in vivo confocal microscopic study. Neuron 1990;5:159–171. [PubMed: 2383399]

Otal R, Martinez A, Soriano E. Lack of TrkB and TrkC signaling alters the synaptogenesis and maturation of mossy fiber terminals in the hippocampus. Cell Tissue Res 2005;319:349–358. [PubMed: 15726425]

Peters, A.; Palay, SL.; Webster, H. The fine structure of the nervous system. New York: Oxford University Press; 1991. p. 494

Pinches EM, Cline HT. Distribution of synaptic vesicle proteins within single retinotectal axons of *Xenopus* tadpoles. J Neurobiol 1998;35:426–434. [PubMed: 9624623]

Poo MM. Neurotrophins as synaptic modulators. Nat Rev Neurosci 2001;2:24–32. [PubMed: 11253356]

Pozzo-Miller LD, Gottschalk W, Zhang L, McDermott K, Du J, Gopalakrishnan R, Oho C, Sheng ZH, Lu B. Impairments in high-frequency transmission, synaptic vesicle docking, and synaptic protein distribution in the hippocampus of BDNF knockout mice. J Neurosci 1999;19:4972–4983. [PubMed: 10366630]

Reh TA, Constantine-Paton M. Retinal ganglion cell terminals change their projection sites during larval development of *Rana pipiens*. J Neurosci 1984;4:442–457. [PubMed: 6607979]

Rodriguez JJ, Davies HA, Silva AT, De Souza IE, Peddie CJ, Colyer FM, Lancashire CL, Fine A, Errington ML, Bliss TV, Stewart MG. Long-term potentiation in the rat dentate gyrus is associated

with enhanced Arc/Arg3.1 protein expression in spines, dendrites and glia. Eur J Neurosci 2005;21:2384–2396. [PubMed: 15932597]

Ruthazer ES, Li J, Cline HT. Stabilization of axon branch dynamics by synaptic maturation. J Neurosci 2006;26:3594–3603. [PubMed: 16571768]

Rybicka KK, Udin SB. Ultrastructure and GABA immunoreactivity in layers 8 and 9 of the optic tectum of *Xenopus laevis*. Eur J Neurosci 1994;6:1567–1582. [PubMed: 7850020]

Sanchez AL, Matthews BJ, Meynard MM, Hu B, Javed S, Cohen-Cory S. BDNF increases synapse density in dendrites of developing tectal neurons in vivo. Development 2006;133:2477–2486. [PubMed: 16728478]

Schikorski T, Stevens CF. Quantitative ultrastructural analysis of hippocampal excitatory synapses. J Neurosci 1997;17:5858–5867. [PubMed: 9221783]

Schikorski T, Stevens CF. Morphological correlates of functionally defined synaptic vesicle populations. Nat Neurosci 2001;4:391–395. [PubMed: 11276229]

Skoff RP, Hamburger V. Fine structure of dendritic and axonal growth cones in embryonic chick spinal cord. J Comp Neurol 1974;153:107–147. [PubMed: 4810722]

Soppet D, Escandon E, Maragos J, Middlemas DS, Reid SW, Blair J, Burton LE, Stanton BR, Kaplan DR, Hunter T, et al. The neurotrophic factors brain-derived neurotrophic factor and neurotrophin-3 are ligands for the trkB tyrosine kinase receptor. Cell 1991;65:895–903. [PubMed: 1645620]

Sorra KE, Fiala JC, Harris KM. Critical assessment of the involvement of perforations, spinules, and spine branching in hippocampal synapse formation. J Comp Neurol 1998;398:225–240. [PubMed: 9700568]

Squinto SP, Stitt TN, Aldrich TH, Davis S, Bianco SM, Radziejewski C, Glass DJ, Masiakowski P, Furth ME, Valenzuela DM, et al. trkB encodes a functional receptor for brain-derived neurotrophic factor and neurotrophin-3 but not nerve growth factor. Cell 1991;65:885–893. [PubMed: 1710174]

Swanwick CC, Harrison MB, Kapur J. Synaptic and extrasynaptic localization of brain-derived neurotrophic factor and the tyrosine kinase B receptor in cultured hippocampal neurons. J Comp Neurol 2004;478:405–417. [PubMed: 15384067]

Tao HW, Poo M. Retrograde signaling at central synapses. Proc Natl Acad Sci U S A 2001;98:11009–11015. [PubMed: 11572961]

Tao HW, Poo MM. Activity-dependent matching of excitatory and inhibitory inputs during refinement of visual receptive fields. Neuron 2005;45:829–836. [PubMed: 15797545]

Tao HW, Zhang LI, Engert F, Poo M. Emergence of input specificity of LTP during development of retinotectal connections in vivo. Neuron 2001;31:569–580. [PubMed: 11545716]

Tashiro A, Dunaevsky A, Blazeski R, Mason CA, Yuste R. Bidirectional regulation of hippocampal mossy fiber filopodial motility by kainate receptors: a two-step model of synaptogenesis. Neuron 2003;38:773–784. [PubMed: 12797961]

Tyler WJ, Pozzo-Miller LD. BDNF enhances quantal neurotransmitter release and increases the number of docked vesicles at the active zones of hippocampal excitatory synapses. J Neurosci 2001;21:4249–4258. [PubMed: 11404410]

Tyler WJ, Pozzo-Miller L. Miniature synaptic transmission and BDNF modulate dendritic spine growth and form in rat CA 1 neurones. J Physiol 2003;553:497–509. [PubMed: 14500767]

Tyler WJ, Zhang XL, Hartman K, Winterer J, Muller W, Stanton PK, Pozzo-Miller L. BDNF increases release probability and the size of a rapidly recycling vesicle pool within rat hippocampal excitatory synapses. J Physiol 2006;574:787–803. [PubMed: 16709633]

Vaughn JE. Fine structure of synaptogenesis in the vertebrate central nervous system. Synapse 1989;3:255–285. [PubMed: 2655146]

Wang X, Butowt R, von Bartheld CS. Presynaptic neurotrophin-3 increases the number of tectal synapses, vesicle density, and number of docked vesicles in chick embryos. J Comp Neurol 2003;458:62–77. [PubMed: 12577323]

Wittig JH Jr, Parsons TD. Synaptic ribbon enables temporal precision of hair cell afferent synapse by increasing the number of readily releasable vesicles: a modeling study. J Neurophysiol 2008;100:1724–1739. [PubMed: 18667546]

Wong WT, Wong RO. Rapid dendritic movements during synapse formation and rearrangement. Curr Opin Neurobiol 2000;10:118–124. [PubMed: 10679440]

Yen LH, Sibley JT, Constantine-Paton M. Fine-structural alterations and clustering of developing synapses after chronic treatments with low levels of NMDA. J Neurosci 1993;13:4949–4960. [PubMed: 8229207]

Yuste R, Bonhoeffer T. Morphological changes in dendritic spines associated with long-term synaptic plasticity. Annu Rev Neurosci 2001;24:1071–1089. [PubMed: 11520928]

Yuste R, Bonhoeffer T. Genesis of dendritic spines: insights from ultrastructural and imaging studies. Nat Rev Neurosci 2004;5:24–34. [PubMed: 14708001]

Zhang LI, Tao HW, Holt CE, Harris WA, Poo M. A critical window for cooperation and competition among developing retinotectal synapses. Nature 1998;395:37–44. [PubMed: 9738497]

Ziv NE, Smith SJ. Evidence for a role of dendritic filopodia in synaptogenesis and spine formation. Neuron 1996;17:91–102. [PubMed: 8755481]

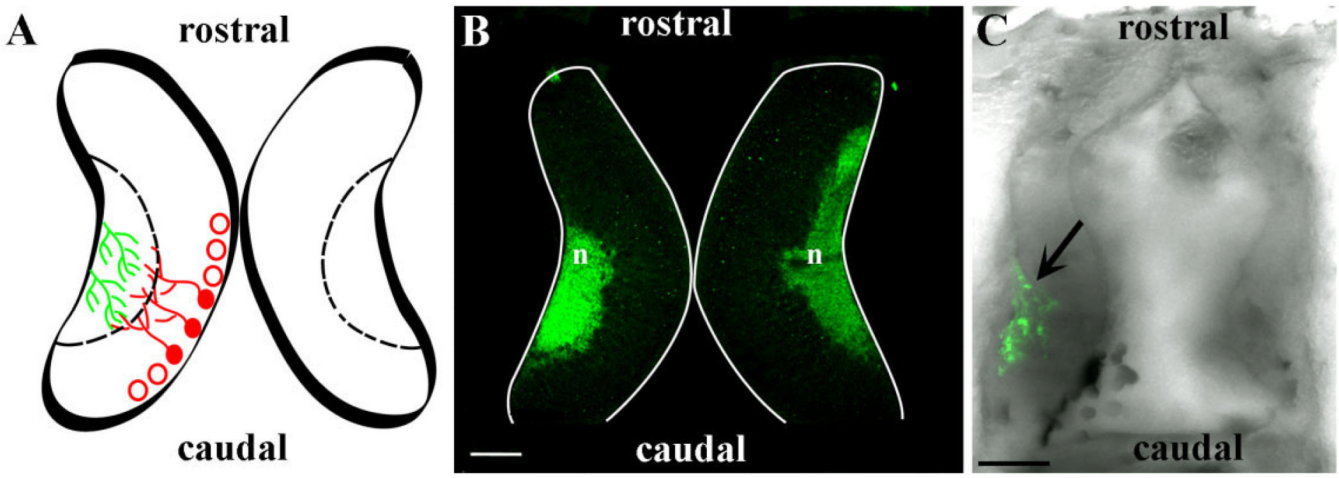

Figure 1.

A: Diagram of the *Xenopus* optic tectum (horizontal view), shows tectal neurons (red) projecting their dendrites to the tectal neuropil and RGC axons (green) branching in the tectal neuropil. **B:** Horizontal section of a stage 45 *Xenopus* midbrain immunostained with an anti-VAMP2 antibody (green immunofluorescence), a presynaptic protein, illustrates the localization of the synaptic tectal neuropil in the lateral portion of the midbrain (n). **C:** Confocal projection of RGC axon arbors in vivo expressing YFP (green fluorescence) that project to, and branch in, the tectal neuropil (phase image). Scale bars = 50 μm in B; 100 μm in C.

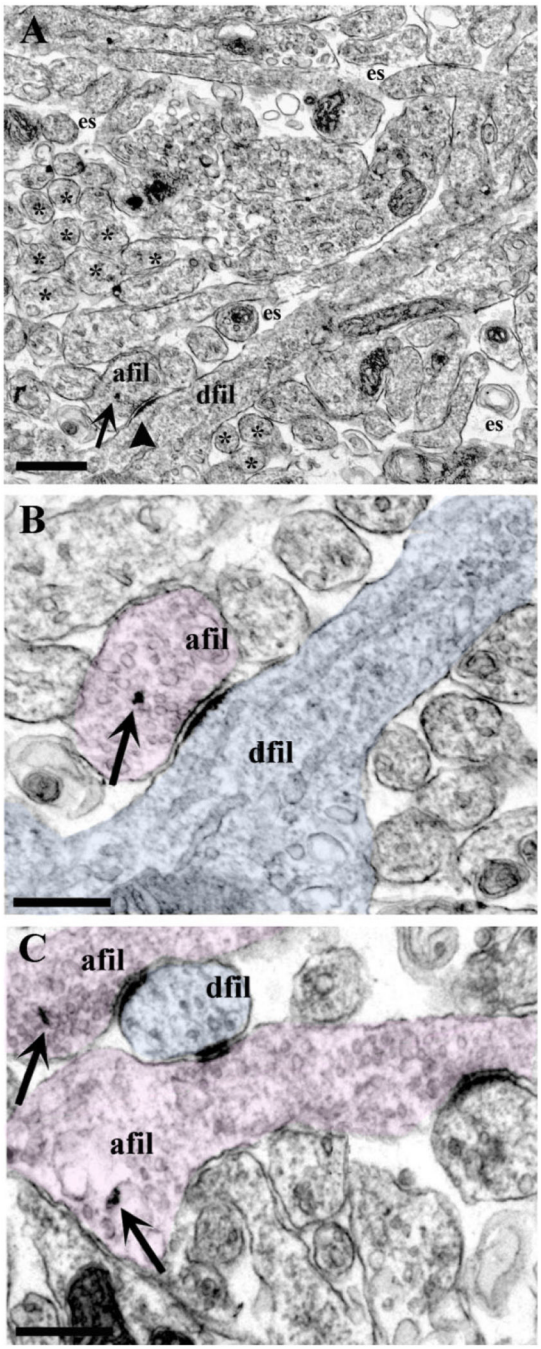

Figure 2.

Ultrastructural organization of the stage 40 *Xenopus* tectal neuropil. Brains of stage 40 tadpoles with RGCs expressing YFP were processed for preembedding immunoelectron microscopy. **A:** Low-magnification electron micrograph of the stage 40 tectal neuropil illustrates the fine structural organization of this tissue at this stage. Note the presence of extracellular space (es) between filopodial-like profiles (asterisks), characteristic of the immature neuropil (Reh and Constantine-Paton, 1984). In cross-section, these small profiles are between 100 and 200 nm. The arrowhead points to the synaptic profile shown in B. **B,C:** YFP-immunopositive axonal filopodial-like profiles (afil; highlighted in pink) make synaptic contacts with their dendritic counterparts (dfil; highlighted in blue). The silver-

enhanced gold particles, marked by the black arrows, identify these presynaptic terminals as those of RGC axons. B corresponds to an enlarged area of the tectal neuropil shown in A. Scale bars = 500 nm in A; 200 nm in B,C.

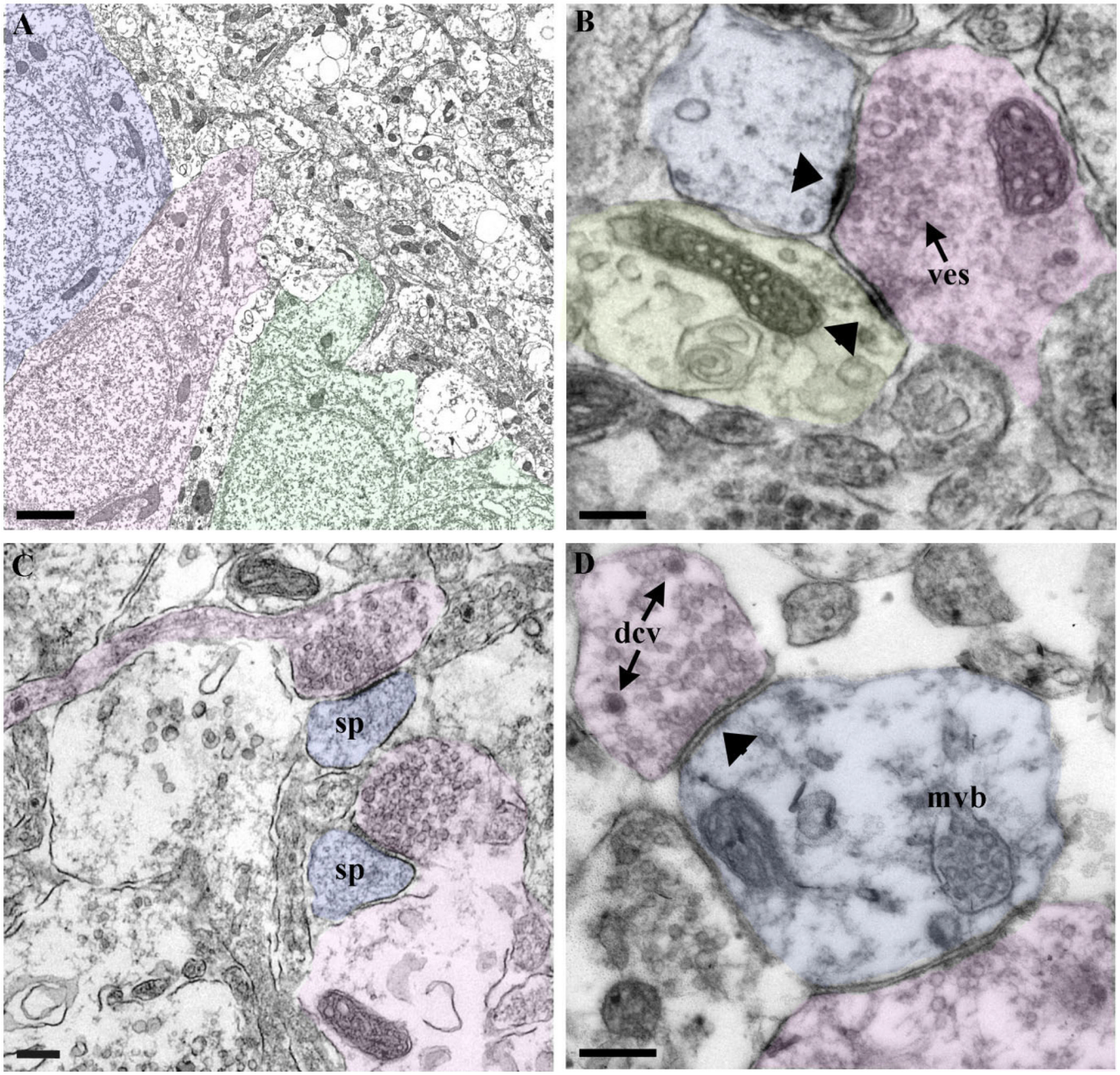

Figure 3.

Ultrastructural organization of the stage 45 *Xenopus* optic tectum. **A:** Low-magnification electron micrograph of the medial portion of the optic tectum shows three neuronal cell bodies positioned adjacent to the tectal neuropil. **B:** Fully mature synapses are established between a presynaptic axon terminal (highlighted in pink) and two postsynaptic dendrites (blue and yellow). Arrowheads point to the postsynaptic densities (ves; synaptic vesicles). **C:** Presynaptic terminals (pink) also establish mature synaptic contacts with dendritic spines (blue). **D:** The presence of dense-core vesicles presynaptically (dcv) and multivesicular bodies (mvb) in postsynaptic terminals (blue) in the developing tectal neuropil is also shown in this sample tissue embedded in LR-white. Scale bars = 2μm in A; = 200 nm in B – D.

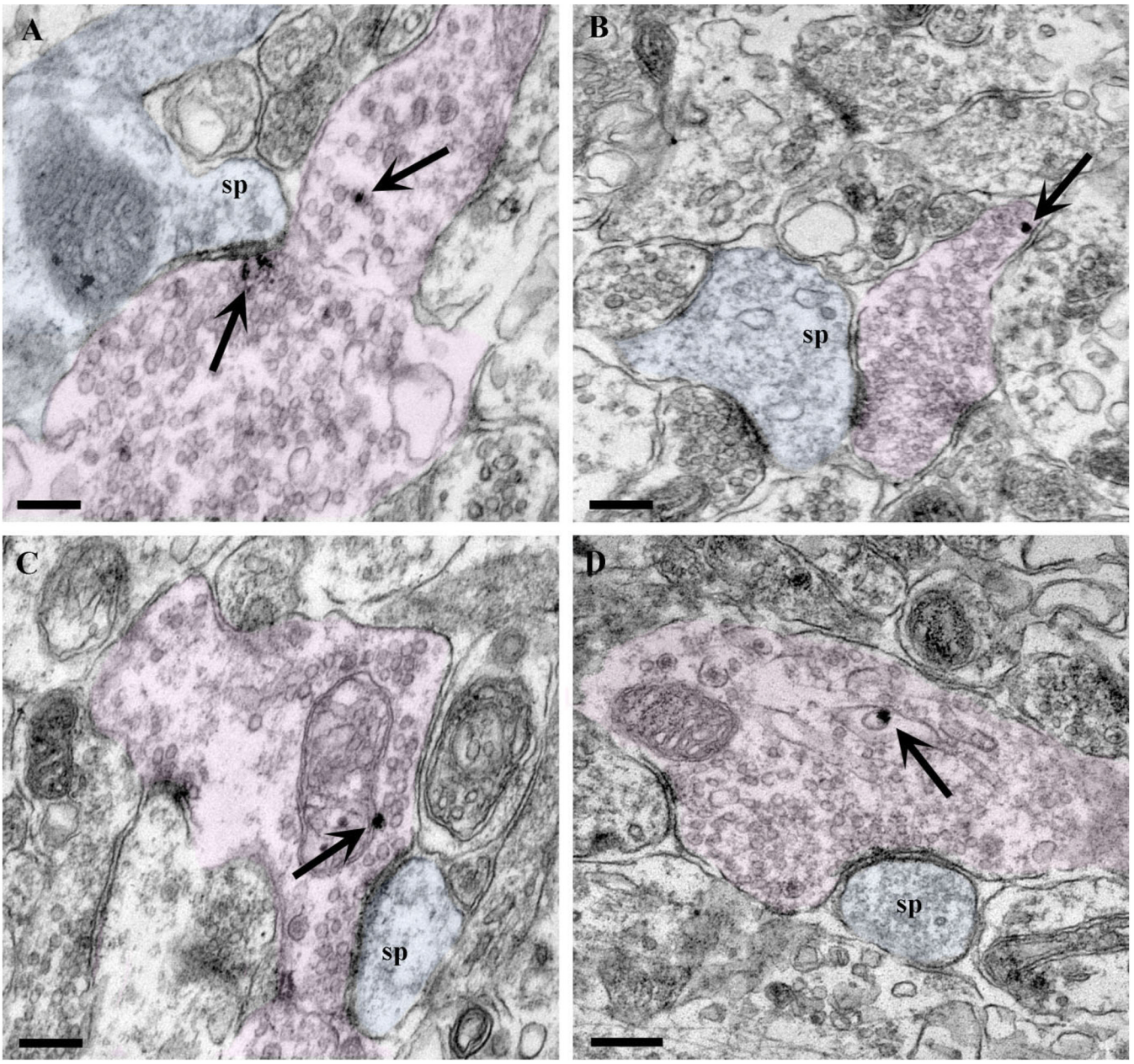

Figure 4.

RGC axon terminals establish synapses with dendritic spines. **A – D:** YFP-immunopositive presynaptic profiles (pink) make synapses with dendritic spines (blue). In all panels, YFP-immunopositive, silver-enhanced gold particles are marked by the arrows. A: In this sample, an axon terminal makes contact with the spine neck. B: A spine receives multisynaptic input; a contact is made by a YFP-positive RGC axon terminal that itself synapses on other dendritic processes. C,D: Examples of YFP-identified RGC axon terminals (pink) that make synaptic contact with dendritic spines (blue). Scale bars = 200 nm.

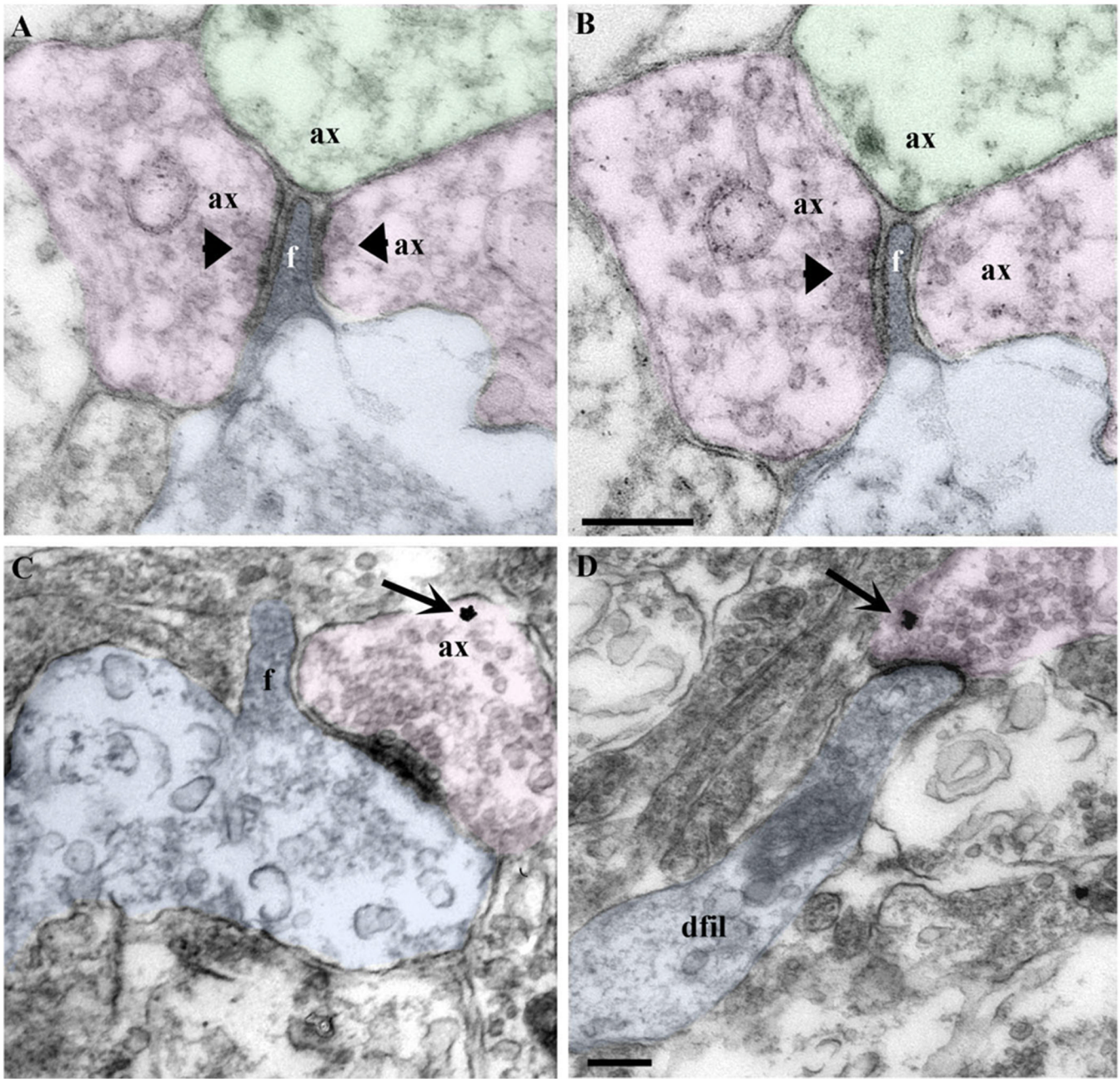

Figure 5.

Filopodial synapses in the stage 45 *Xenopus* optic tectum. **A,B:** Serial ultrathin sections show a nascent dendritic filopodium (blue) that receives synaptic input (arrowheads) from multiple presynaptic terminals (pink). A nonsynaptic terminal containing a few synaptic vesicles (green) also contacts this filopodium. **C,D:** RGC axon terminals (pink) labeled with YFP and identified by gold particle immunoreactivity (arrows) establish synaptic contacts with a filopodia-bearing (f) growth cone-like structure (blue) in C, and with dendritic filopodial-like profiles (dfil; blue) in D. Dendritic filopodia-like profiles can receive multiple synaptic contacts (A) or can receive a single synaptic input from a presynaptic fiber (D). Scale bars = 200 nm in B (applies to A,B); 200 nm in D (applies to C,D).

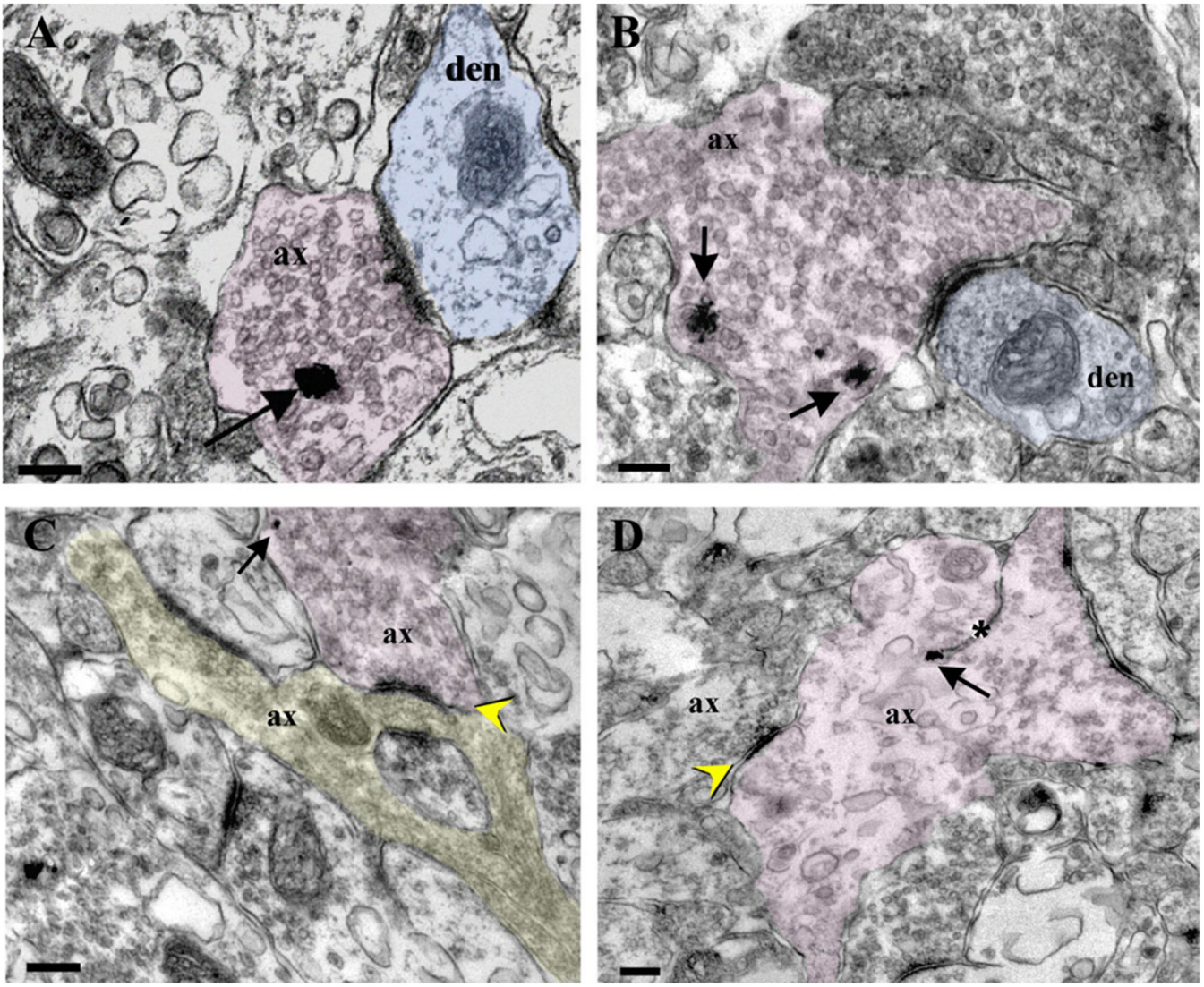

Figure 6.

Shaft and axoaxonal synapses in the *Xenopus* optic tectum. **A,B:** Synapses between YFP-immunopositive RGC axon terminals (pink) and tectal neuron dendrites at a shaft (blue) are illustrated in these sections of the stage 45 tectal neuropil. **C,D:** Axoaxonal synaptic profiles are also found in the stage 45 *Xenopus* tectal neuropil. C: An RGC axon (pink) expressing YFP (arrow) makes synaptic contact with an axonal terminal (highlighted in yellow). D: In this sample, a YFP-identified RGC axonal profile (pink) receives axoaxonal input from a neighboring axon (yellow arrowhead). A spinule, a thin projection of cytoplasm and membrane of the dendritic surface that divide a presynaptic bouton (Sorra et al., 1998), is marked by the asterisk. In all panels, the silver-enhanced YFP immunogold particles are marked by arrows. ax, Axon terminal; den, dendritic profile. Scale bars = 200 nm.

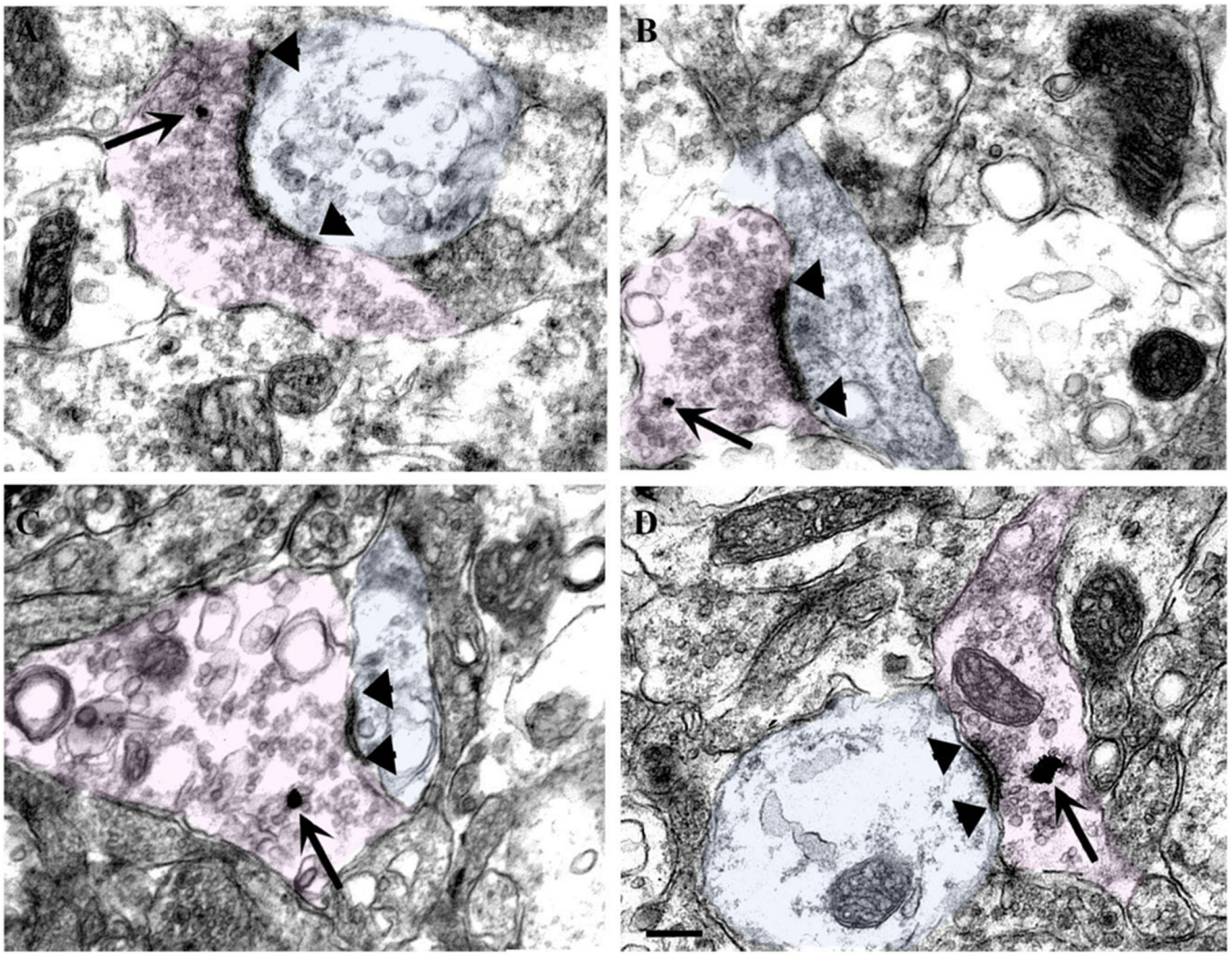

Figure 7.

Enlarged active zone at retinotectal synapses in the tectal neuropil of BDNF-treated tadpoles. **A,B:** Immunoelectron micrographs of the tectal neuropil of tadpoles with RGC axons expressing YFP (arrows), 8 hours following tectal injection of BDNF. **C,D:** Electron micrographs of tectal neuropil of control, stage 45 tadpoles with RGC axons expressing YFP (arrows). Note that the lengths of the presynaptic active zone and the corresponding postsynaptic densities (arrowheads) are larger at YFP-identified retinotectal synapses in the BDNF-treated tadpoles (A,B) than in control-treated tadpoles at the same stage (C,D). Scale bar = 200 nm.

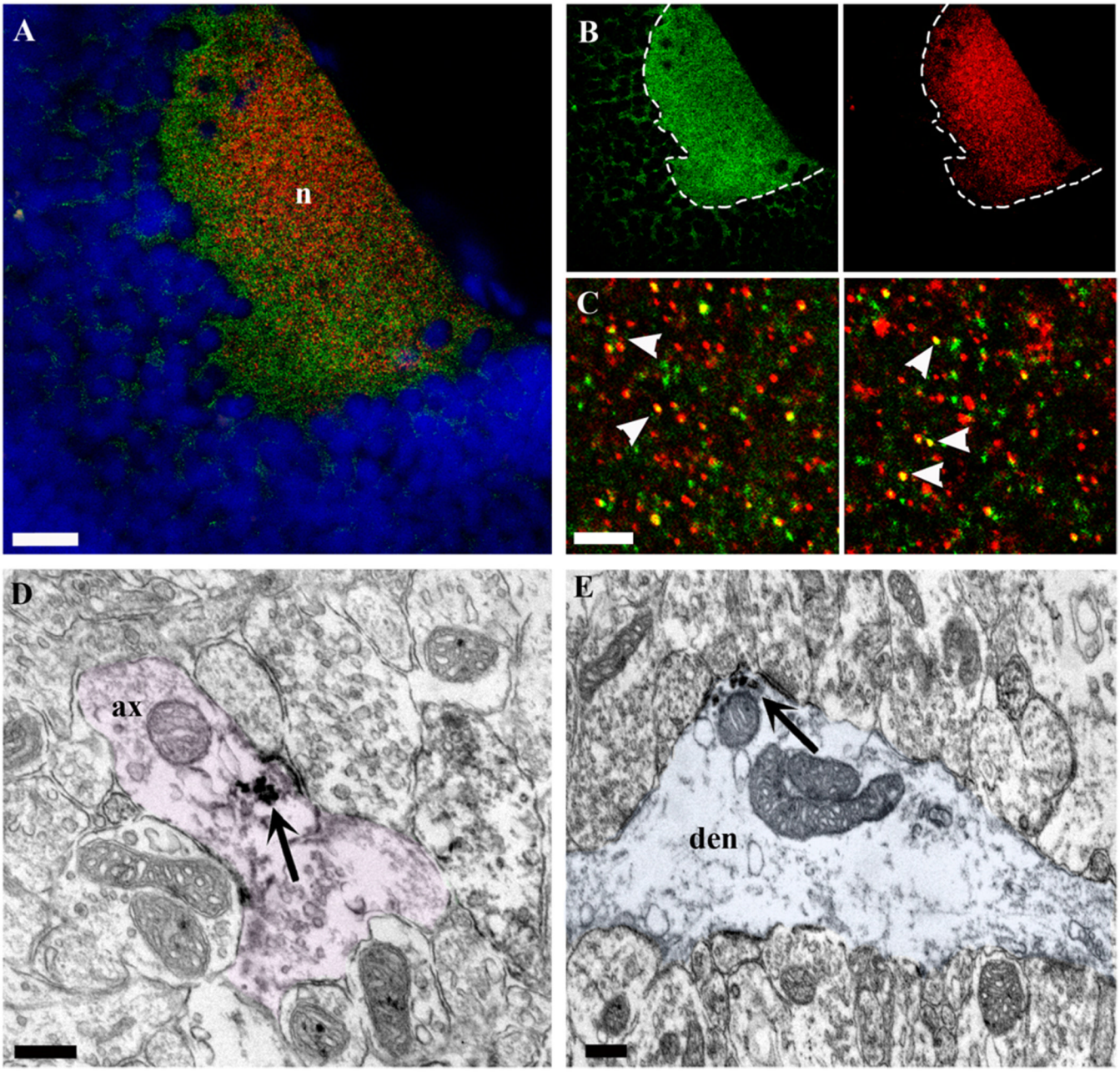

Figure 8.

Cellular and subcellular distribution of full-length TrkB in the stage 45 *Xenopus* optic tectum. **A,B:** Coronal section of a stage 45 *Xenopus* midbrain at the level of the optic tectum shows the distribution of TrkB immunoreactivity (green fluorescence) in the tectal neuropil (n) and its colocalization with the presynaptic marker SNAP-25 (red fluorescence). In A, the cell body layer is shown by DAPI fluorescence (blue). **B:** The distribution of TrkB immunofluorescence in the neuropil and surrounding cell bodies near the neuropil is better illustrated by separating the two channels, in which TrkB alone (green) and SNAP-25 (red) localization are shown. The border between the cell body layer and the tectal neuropil is demarcated by the dashed line. **C:** Thin, horizontal, high-magnification confocal sections show the colocalization of TrkB (green) and SNAP-25 (red) immunofluorescence at the

level of the tectal neuropil. **D,E:** Immunoelectron microscopy illustrates the subcellular distribution of TrkB in the tectal neuropil. The immunoperoxidase reaction product (arrows) reveals that TrkB immunoreactivity localizes to axon terminals (D, pink) as well as dendritic profiles (E, blue). In E, a large-caliber dendrite that receives multiple synaptic contacts contains TrkB-immunoreactive precipitate near the postsynaptic membrane (arrow). For a green-magenta version of parts of this figure see Supporting Information Figure 4. Scale bars = 50 μm in A; 5 μm in C; 200 nm in D,E.

TABLE 1

Primary Antibody Information

Antibody	Immunogen	Source/species in which raised/catalog No.	Dilution
TrkB (*Xenopus*, full-length)	Synthetic peptide; amino acid residues 396–411 of the cytoplasmic domain of *Xenopus* TrkB (LQNLSKASPVYLDILG)	Bethyl Laboratories Inc. (Montgomery, TX) rabbit polyclonal custom-made	1:2,000
GFP	Green fluorescent protein purified from *A. victoria*	Invitrogen (Eugene, OR) mouse monoclonal (IgG_{2a}), clone 3E6 catalog No. A11120	1:10
3A10 mouse monoclonal antibody	Generated in mice against chicken nervous tissue; recognizes a neurofilament-associated antigen in *Xenopus* RGCs (Hocking et al., 2008; Manitt et al., 2009) and spinal cord neurons (Gravagna et al., 2008)	Developed by Drs. T. Jessell and J. Dodd (Columbia University), and obtained from the Developmental Studies Hybridoma Bank[1] mouse monoclonal (IgG_1) catalog No. 3A10	1:2,000
SNAP-25	Raised against synaptic vesicle-containing fractions immunoprecipitated from human brain homogenates using anti-human synaptophysin monoclonal antibodies	Assay Designs (Ann Arbor, MI) mouse monoclonal (IgG_1), clone SP12 catalog No. VAM-SV0012	1:1,000
VAMP2	Raised against a highly conserved peptide sequence of rat VAMP2 (residues 36–56) (QAQVDEVVDIMRVNVDKVLER)	Assay Designs (Ann Arbor, MI) rabbit polyclonal catalog No. VAS-SV006	1:1,000

[1] Developed under the auspices of the NICHD and maintained by The University of Iowa, Department of Biological Sciences, Iowa City, IA 52242.

TABLE 2

Classification of YFP-Identified Retinotectal Synapses in the Stage 45 *Xenopus* Tectal Neuropil 24 Hours After Treatment[1]

	Axoaxonal (%)	Axodendritic (%)	On filopodia (%)	On spines (%)
Control (n = 104)	3.52 ± 1.85	40.36 ± 6.88	47.55 ± 6.7	8.55 ± 4.56
BDNF (n = 101)	1.76 ± 1.77	36.92 ± 5.47	31.50 ± 8.9	29.8 ± 4.63[2]

[1] In total, 11 brains were analyzed for controls and nine for BDNF-treated tadpoles. The relative proportion of each synaptic profile type was determined for each tadpole brain. Data represent the average obtained for all tadpoles per individual treatment and are expressed as percentage of total; n = number of synaptic terminals analyzed.

[2] $P = 0.0048$.

TABLE 3

Number and Density of Synaptic Vesicles per Profile (N/μm^2), Number of Docked Synaptic Vesicles (N/μm), and Length of the Active Zone (Postsynaptic Density; in nm) in YFP-Identified Retinotectal Synapses in Controls and BDNF-Treated Tadpoles[1]

	Control	BDNF 8 hours	BDNF 24 hours
Mature synaptic profiles (%)	46.3 ± 4.2	40.43 ± 4.35	60.25 ± 3.9[2]
Synaptic vesicle number	66.95 ± 11.13	63.49 ± 5.1	68.39 ± 4.5
Synaptic vesicle density (per μm)	18.8 ± 2.9	19.54 ± 3.052	22.25 ± 2.85
Number of docked vesicles	6.46 ± 0.46	7.423 ± 0.58	8.15 ± 0.52[3]
Length of active zone (nm)	206 ± 10	290 ± 19[4]	225 ± 12

[1] Number of YFP-immunopositive synaptic profiles analyzed for each individual treatment is n = 80 for controls, n = 69 for BDNF 8 hours, and n = 71 for BDNF 24 hours. One-way ANOVA was used for the statistical analysis of data.

[2] $P = 0.049$ compared with controls.

[3] $P = 0.0162$ compared with controls.

[4] $P = 0.0046$ compared with BDNF 24 hours and $P < 0.0001$ compared with controls.